n94

N90-22100

ON THE DESIGN AND DEVELOPMENT OF A MINIATURE CERAMIC GIMBAL BEARING

by Robert A. Hanson*, Barry O'Dwyer*, Keith M. Gordon*, and Edward W. Jarvis*

ABSTRACT

A review is made of a program to develop ceramic gimbal bearings for a miniaturized missile guidance system requiring nonmagnetic properties and higher load capacity than possible with conventional AISI 440C stainless steel bearings.

A new gimbal design concept is described which utilizes the compressive strength and nonmagnetic properties of silicon nitride (Si_3N_4) ceramics for the gimbal bearing. Considerable manufacturing development has occurred in the last five years making ceramic bearings a viable option in the gimbal design phase. Bearings with Si_3N_4 races and balls are now manufactured and available in several miniature sizes ranging from size 518, 3.2 mm bore x 7.9 mm OD (0.125 in x 0.3125 in), to size R8, 12.7 mm bore x 28.5 mm OD (0.500 in x 1.125 in). The design also utilizes a unique bearing design to overcome some of the inherent limitations of the ceramic material and adhesive assembly of the gimbal to simplify the manufacturing procedure.

This paper summarizes a preliminary study into the feasibility of the proposed design. Finite element analyses of the brittle ceramic bearing components under thermal stress and high acceleration loading were conducted to ensure the components will not fail catastrophically in service. Finite element analysis was also used to optimize the adhesive joint design. Strength tests on several candidate adhesives indicate that adhesives are available that provide adequate adhesive joint strength between the metal gimbal ring and the ceramic bearing rings. Bearing torque tests run at various axial loads indicate that the average running torque of ceramic bearings varies with load similarly to that of conventional steel bearings. Axial compliance (deflection vs load) tests indicate that the ceramic bearings are, not unexpectedly, somewhat stiffer than steel bearings. Preliminary results indicate the new design concept, utilizing ceramic gimbal bearings, is a viable option and further, more detailed study is warranted.

*Miniature Precision Bearings, Division of MPB Corp., Keene, NH

INTRODUCTION

The gimbal miniaturization program was initiated to develop an improved performance guidance system for an air-to-air missile which presents some serious gimbal bearing design problems. In particular, the design requires a nonmagnetic bearing material, high load capacity (necessary to survive the high acceleration forces of launch without Brinell damage to the raceways), and a tiny size 2.5 (1.2 mm bore) bearing is the largest that fits into the available space.

Table 1 - Required Load Capacity

Direction	N	lb
Radial	38.7	8.7
Axial	25.8	5.8

The miniaturization of the gimbal system reduced the diameter of the gyroscope drive motor magnet and coil, located outside the gimbal, making them closer to the gimbal bearings, thus exposing the current 440C stainless steel bearings to much stronger magnetic fields. The stronger fields result in significant magnetic attraction of the ferromagnetic bearings effecting the freedom of movement of the gimbal by magnetic drag. In tests, the traditional nonmagnetic bearing material, 2 % beryllium copper (copper alloy 172), eliminated this problem, but does not have adequate load capacity. The maximum acceptable Hertz contact stress for beryllium copper is much lower than 440C. In fact, the original 440C steel bearing had only marginal load capacity in the application.

Si_3N_4 bearings provide an interesting alternative since they are nonmagnetic and have higher load capacity than bearings made from either beryllium copper or 440C. Si_3N_4 has demonstrated superior bearing performance in many tests over the last 20 years. Its capabilities are well documented. Although the bearing is smaller than any monolithic all-ceramic ball bearing ever manufactured that we are aware of, it is a feasible project from a manufacturing standpoint, based on recent ceramic manufacturing developments.

A problem arises, however, with the design - conventional gimbal systems are designed with flanged outer ring gimbal bearings (never before attempted in ceramics and complicated by the tiny size of the components) and the gimbal bearing inner ring is mounted on the internally threaded trunnion of the inner gimbal and secured by a screw, as shown in Figure 1. Si_3N_4 has a low thermal expansion coefficient compared to the metals used for the gimbals, here Inconel 600, which would result in potentially damaging tensile hoop stresses on the inner ring at elevated temperatures. Si_3N_4 has a relatively low tensile strength and is subject to catastrophic brittle failure if the applied loads exceed the strength of the inner ring. A conventionally designed Si_3N_4 gimbal bearing, although it would be nonmagnetic and have improved load capacity, would be potentially very difficult to manufacture and subject to inner ring fracture at elevated temperatures. In addition, the bearing bore and OD and bearing mounting surfaces on the gimbals are precisely matched fits requiring ultra-precision machining which gets more difficult as the gimbals are miniaturized.

Table 2 - Thermal Expansion Coefficients		
Temperature Range: -54 to 123°C (-65 to 253°F)		
	/°C	(/°F)
Inconel 600[1]	12.6×10^{-6}	(7.0×10^{-6})
Si_3N_4[2]	0.97×10^{-6}	(0.54×10^{-6})

For many reasons it was desirable to develop a gimbal system design that allowed the use of ceramic bearings and also improved the manufacturability of the gimbals. A new design concept, Figure 2, was suggested that fixed the bearing rings to the gimbals with adhesives, rather than mechanically. This eliminated the need for the bearing outer ring flange and reduced the required precision of the gimbal mounting surfaces. The alignment of the proposed gimbal bearing can be adjusted during assembly of the gimbal, before the adhesive has cured.

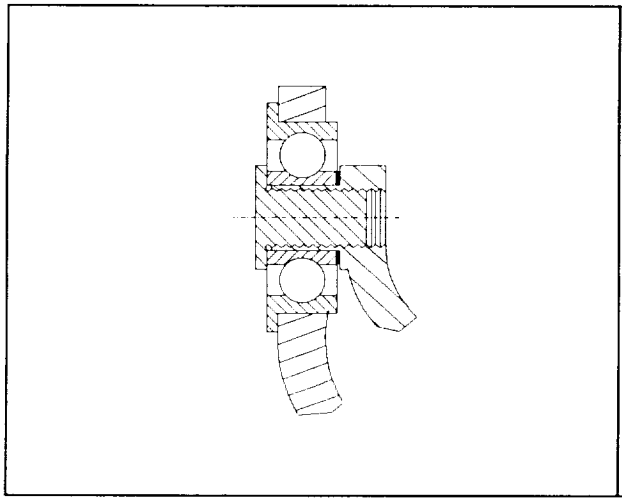

Figure 1: Conventional design

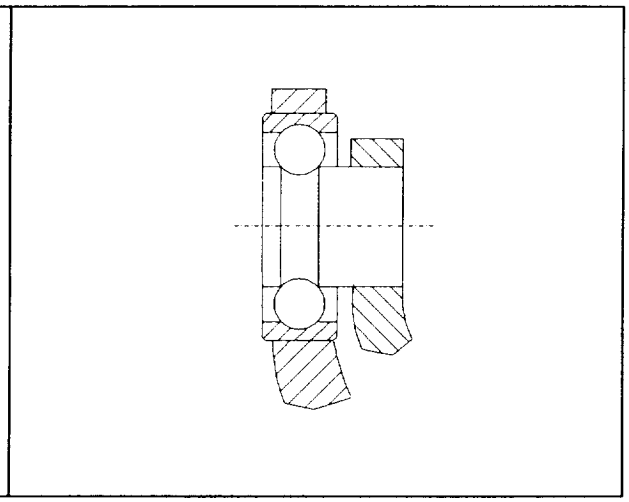

Figure 2: New concept

The bearing inner ring for the new concept design is a solid pin which is inserted in a mounting hole in the inner gimbal. This eliminates the risk of brittle tensile failure of the inner ring due to tensile stresses from a metal shaft that expands faster than the ceramic inner ring.

Another advantage of the new design is that, without the requirement for an outer ring flange for mounting, it allowed space for a somewhat larger bearing with additional load capacity.

CERAMIC MATERIALS

Cerbec NBD-100 (HIP) material was selected for the races and NC-132 (HP) for the balls based on extensive experience with the materials in the bearing industry as a whole and, more importantly, within MPB. Both materials have been well characterized by Cerbec

and others. Since the program is a rapidly evolving design with little time for prototype manufacturing, availability was also a crucial concern. NBD-100 race blanks and NC-132 balls were both readily available.

Ceramic materials do not significantly deform plastically under loads, as most metals do, but fail by brittle fracture at defects in the material. The probability of failure at a point is the combination of the calculated stress at that point and the probability of exposing a defect large enough to cause brittle failure at that stress. There is some finite chance that a defect in a low-stressed area may be large enough to initiate the failure there before it is initiated in a high-stressed zone. For this reason one must evaluate the probability of failure over the whole volume of the ceramic component, not only the highest stressed region, to determine the reliability of the component under load. Our preliminary study did not evaluate the probability of failure of each area of the component, only the highest stressed region. Further studies must be conducted to do this if the initial results are encouraging.

Furthermore, one must stress a large volume of material in strength tests on ceramics to get a good assessment of the probability of having damaging defects in a particular material lot. The reliability of the strength data depends directly on the volume of material stressed in the test and the number of samples tested. These two criteria define the sample size, that is the total volume of material tested. If the strength data does not have a high confidence level, the ceramic parts must be oversized or the loads reduced to give adequate reliability.

The Weibull plot representing the four point bending strength of the Cerbec NBD-100 done as a qualification test on a recent lot of material is shown in Figure 3. [2] There were 16 test specimens made in accordance with MIL-STD-1942B. The average failure load is 782 MPa (113 kpsi) and the Weibull modulus is 8.2. It should be pointed out that this is a conservative estimate for our use since the stressed area in this test is quite large, 4 mm x 20 mm, compared to the size of our components. It also should be noted that these tests, representing one lot only, may be somewhat different from other data that has been reported on this material.

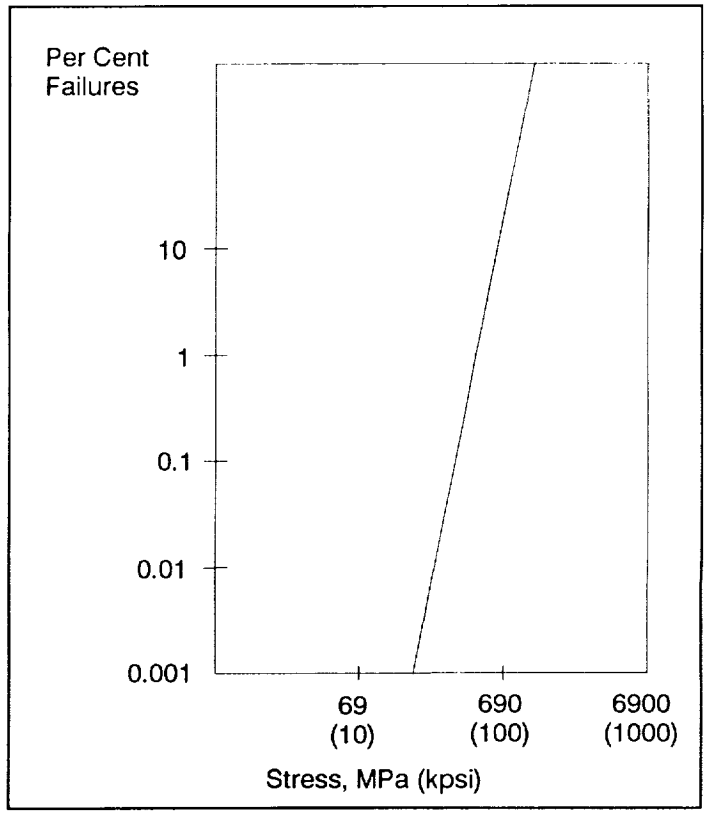

Figure 3: Four-point bending strength of NBD-100

LOAD CAPACITY

The conventional definition of bearing static load capacity of miniature and instrument bearings is the maximum load at which the maximum Hertz stress on the heaviest loaded raceway under the heaviest loaded ball will not cause significant permanent deformation, or fracture in the case of ceramics, or the maximum load at which the contact ellipse does not intersect the raceway/land corner. Generally radial load capacity is determined by the former criteria and axial load capacity by the latter.

The rating stress for 440C is specified by the AFBMA as 4,000 MPa (580 kpsi). [3] This value was determined by statically loading bearings at various levels and torque testing to find the point where the Brinells became apparent on the torque traces. The rating stress for BeCu can be estimated from the yield strength, 1,255 MPa (182 kpsi), by assuming the same relationship between yield strength and rating stress as was determined for 440C.

Si_3N_4, however, does not significantly plastically deform under load, it fractures once the stress limit is reached. The load capacity criteria for Si_3N_4 bearings must, therefore, be determined by a different method. No standard method has been established yet, but the general practice is to estimate the static load capacity from measured compressive fracture strength data. (In actuality the Si_3N_4 does not fail in the compressive stressed contact area, but in the tensile stressed zone immediately outside the contact zone.) Fujiwara et al. used acoustic emission to determine the fracture point in ball-on-plate tests and arrived at failure stresses of 11,000 - 13,800 MPa (1,600 - 2,000 kpsi). [4] Others have estimated the compressive fracture strength at 13,800 - 27,600 MPa (2,000 - 4,000 kpsi) using ball crush tests and ball-on-plate tests. [5,6] The rating stress of the Si_3N_4 for the purposes of this study was determined to be 6,900 MPa (1,000 ksi).

The calculated static load capacity of the bearings is given in Table 3. When compared with the required load capacity (Table 1), all three bearings have adequate axial load capacity, but only the Si_3N_4 bearing has adequate radial load capacity with some margin for safety.

Table 3 - Static Load Capacity

Bearing Description	Radial[a]	Axial[a]	Rating Stress[b]
Size 2.5 440C	39.1 (8.8)	105 (23.7)	4,000 (580)
Size 2.5 BeCu	30.2 (6.8)	82.7 (18.6)	2,650 (384)
Size 3 Si_3N_4	65.4 (14.7)	110 (24.8)	6,900 (1,000)

[a] Load capacity expressed as N/(lb)
[b] Rating stress expressed as MPa/(kpsi)

It should be noted that bearing design variables such as contact angle, the number and size of balls, and raceway curvature can significantly affect the load capacity. Some of these features are specified in table 4.

Table 4 - Bearing Design Features

Bearing Description	ID[a]	OD[a]	Width[a]	# Balls	d (ball)[a]
Size 2.5 440C	1.194 (0.047)	3.962 (0.156)	1.600 (0.063)	10	0.787 (0.031)
Size 2.5 BeCu	1.194 (0.047)	3.962 (0.156)	1.600 (0.063)	10	0.787 (0.031)
Size 3 Si_3N_4	none[b]	4.775 (0.188)	1.372 (0.054)	6	1.000 (0.039)

[a] Dimensions are mm/(in)
[b] There was no bore in the inner ring of this bearing. A standard size 3 bearing has an ID of 1.397 mm (0.055 in).

The radial load capacity of all the bearings in the table was enhanced by using tighter-than-normal race curvatures at the sacrifice of increased torque. The 440C and BeCu bearings listed in Tables 3 and 4 also were of full complement design (i.e., without retainers or ball separators), further enhancing the load capacity by providing more balls, therefore more ball contacts to carry the load, also at the expense of torque performance. The Si_3N_4 bearings, on the other hand, have a retainer and fewer balls which should reduce bearing torque.

ADHESIVE JOINTS

One of the primary concerns with the new design was the adequacy of the adhesive joints. The surfaces of the pins and gimbal bearing seats are very smooth, making adhesion more difficult. It was undesirable to roughen these precision, smooth surfaces to enhance adhesion since roughening operations might reduce the precision of the components, may reduce the bending strength of the Si_3N_4 pin, and cause damage to the inner raceway. The joints must withstand thermal excursions and severe vibration in service.

A pin/gimbal ring joint test piece consisting of a simulated section of the gimbal and a straight cylindrical pin, shown in Figure 4, was designed for adhesive strength tests. The test piece provides a relatively simple and inexpensive test bed that closely

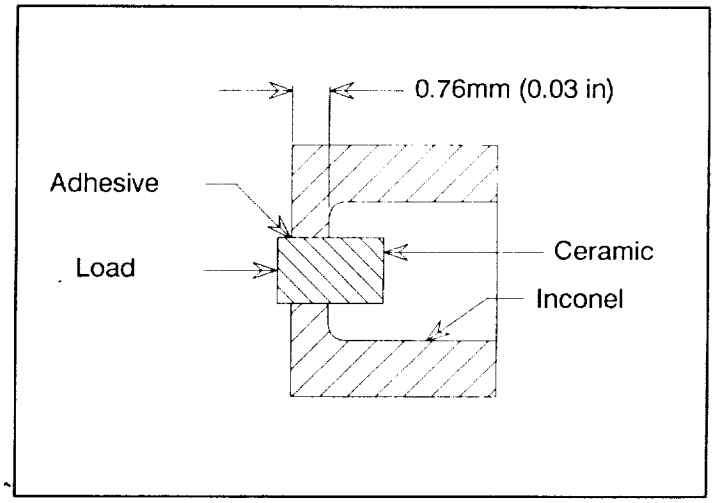

Figure 4: Adhesive strength test piece with applied loads

approximates the actual pin/gimbal joint for evaluation of adhesives, joint clearances, pin OD and gimbal seat surface finishes, etc. The gimbal test piece was thicker than the gimbal ring to make it strong enough to support the projected adhesive joint failure loads. The joint region was reduced in thickness to match the thickness of the gimbal ring.

Six candidate adhesives were selected based on recommendations of others with experience in the field, from adhesives manufacturers, and from manufacturers' data sheets.

Shear tests on the adhesive joint were conducted at room temperature to select the strongest adhesives for further development. The maximum shear load on the adhesive joint in service is estimated to be 122 N (27.5 lb). An initial diametral joint clearance of 0.0051 mm (0.0002 in) was used. A cross-head speed of 5 mm/min (0.200 in/min) was selected. Since the tests are time consuming and the components expensive and in short supply, it was decided to reduce the candidates to two or three as early as possible. The shear test results are given in Table 5. The results were clearcut with three adhesives performing well and three performing poorly. Adhesives A, B, and C, listed in Table 6, were selected for further tests, while adhesives D, E, and F were dropped from the program as being too weak to be suitable.

The smooth surfaces on the pin and gimbal seat did not reduce the adhesion strength of the joint to unacceptable levels. Further manufacturing operations to roughen the surfaces for improved adhesion are, therefore, unnecessary.

It is possible that different test conditions might have improved the performance of adhesives D, E, and F. Since our mission was to find a suitable adhesive for this application, not to study adhesives in general, we did not investigate this possibility.

Table 5 - Adhesive Joint Shear Failure Load[a]

Adhesive	Average	Range
A	331 (74.4)	279-363 (62.7-81.5)
B	328 (73.8)	306-365 (68.8-82.1)
C	282 (63.5)	266-299 (59.8-67.3)
D	66.3 (14.9)	61.8-70.7 (13.9-15.9)
E	29.4 (6.6)	14.7-68.5 (3.3-15.4)
F	18.7 (4.2)	11.6-28 (2.6-6.3)

[a] Failure load expressed as N/(lb)

Table 6 - Strongest Candidate Adhesives	
Aremco Bond 631	(Aremco Products,Inc)
Master Bond EP30	(Master Bond, Inc)
Hysol 956	(Dexter Adhesives and Structural Materials Div)

Further shear strength tests must be conducted at room temperature after cycling the joints to the temperature extremes, -54 and 123°C (-65 and 253°F), at the temperature extremes after long soaks at those temperatures, and after severe vibration. Preliminary temperature cycling tests on two of the three adhesives show the joint strength was reduced 10 - 20 % after five temperature cycles, retaining adequate strength. Longer exposures at the temperature extremes, more temperature cycles, and strength tests at the temperature extremes are necessary to properly test the design.

A finite element analysis of the joint was conducted assuming several diametral adhesive joint clearances from 0.0051 to 0.1270 mm (0.0002 to 0.0050 in) to evaluate the effect of the joint thickness on the tensile stresses on the ceramic pin, at cold temperatures. Since the metallic gimbal seat shrinks much faster than the ceramic pin, the encapsulated portion of the pin is subject to compressive stress, but the surface of the portion of the pin just outside the joint is subject to tensile stress. The polymer adhesive joint acts as a buffer between the two components, reducing the stress. Figure 5 shows the relationship between the diametral joint clearance and the resulting maximum principal stress on the ceramic pin at the highest stressed point at the low temperature extreme. The model assumes the pin is centered in the gimbal seat which, of course, may not be the case in actual gimbal assemblies.

The analysis indicates that joint diametral clearances of 0.01 mm (0.0004 in) and greater reduce the tensile stress at the highest stressed area to below 166 MPa (24 kpsi) and improves the reliability (considering only the highest stress region) to 99.999%. This clearance would also be considered a practical minimum to provide some alignment capability during the gimbal assembly.

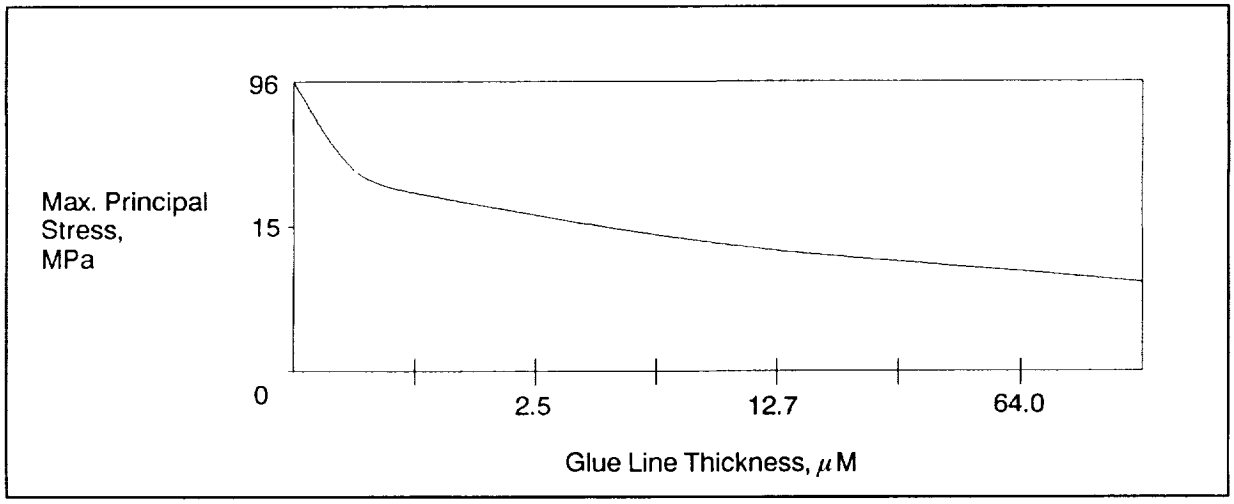

Figure 5: Maximum principal shear stress on pin vs. adhesive diametral joint clearance

PIN STRENGTH

The maximum estimated bending load on the inner ring/pin, seen during launch, is 122 N (27.5 lb). The ceramic pin must be designed to survive these loads. Although Si_3N_4 is very strong in compression, it is relatively weak in tension. Overstress leads to brittle fracture, and in this case catastrophic failure of the system. Finite element analysis of the pin/gimbal joint with the maximum design moment load results in a maximum principal stress on the pin OD near the joint of 173 MPa (25 kpsi).

The strength of the pin appears to be sufficient to support the large launch moment load without failure at least 99.999 % of the time, which is sufficient reliability for the preliminary design. Although this concern needs further study, the initial indications are that the design is adequate.

BEARING TORQUE

Low and consistent bearing torque is important to the proper performance of gimbal systems. Until actual test bearings of the new design are available the torque characteristics of the new bearing cannot be determined. However, the effect of axial load on bearing torque of 440C steel and Si_3N_4 bearings can be determined on other miniature bearings as a guideline.

Standard 440C and Si_3N_4 bearings of three common sizes were evaluated for running torque on an MPB RT2C torque tester at axial loads varying from 4.5 - 67 N (1 - 15 lb) on bearing sizes R2, R3, and R6.

Table 7 - Torque Test Bearing Dimensions[a]

Bearing Size	ID	OD	Width
R2	3.175 (0.125)	9.525 (0.375)	3.967 (0.156)
R3	4.763 (0.188)	12.700 (0.500)	3.967 (0.156)
R6	9.525 (0.375)	22.225 (0.875)	5.558 (0.219)

[a] Dimensions expressed in mm (in)

The average running torque vs axial load results for the R2 bearing size are shown graphically in Figure 6. The average running torque is defined in MIL-STD-206 as one half the average torque difference between consecutive clockwise and counter-clockwise torque traces on the same bearing. It can be seen that the slopes of the lines are approximately parallel, with the ceramic bearing torque being somewhat higher. The higher torque level of these ceramic bearings is probably related to the quality of the races, which are not as high in quality in terms of race finish and race curvature control as the comparable 440C races.

The finishing of ceramic bearing races has undergone significant advancement in the last year and the samples tested do not have the benefit of these improvements.

Of particular interest is the slope of the torque vs axial load lines, which are essentially the same for both 440C and Si_3N_4. This means as the bearings are loaded in service the torque response of the ceramic bearings will be similar to currently used 440C bearings.

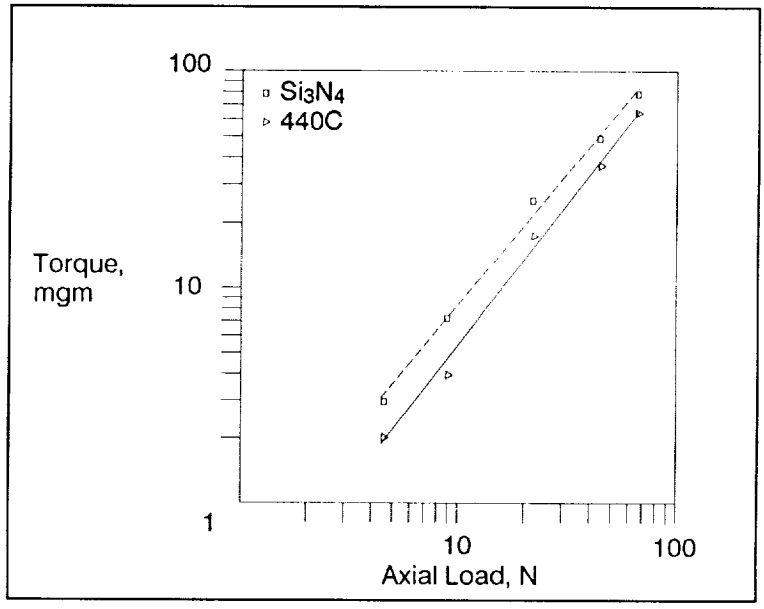

Figure 6: Average running torque vs. axial load for R2 bearings

In addition, the slopes of the logarithmic plots of all the torque vs axial load lines is reasonably close to 1.33. This has been the generally accepted relationship in the instrument bearing industry for many years. That is:

$$T \alpha F_a^{x} \qquad [1]$$

where: T = Average running torque
F_a = Axial load
x = Torque / load exponent

In this case:

$$T \alpha F_a^{1.33} \qquad [2]$$

Table 8 - Torque/Load Exponent (x)			
Material	R2	R3	R6
440C	1.31	1.54	1.21
Si_3N_4	1.22	1.29	1.30

BEARING COMPLIANCE

Bearing compliance (displacement under force) is critical to gimbal design since the stiffer the gimbal the more resistant the system is to drift when exposed to acceleration. The bearings are the "softest" component in the gimbal, hence any improvement in stiffness or compliance of the bearings can have a significant effect on the gimbal system.

Axial deflection tests were run using the MPB axial deflection gage on the same three sets of bearings used for the torque tests. Table 9 gives the slope of the load/deflection curve at a load close to the rated load. The Si_3N_4 clearly provides a stiffer bearing than the standard 440C bearing.

Table 9 - Bearing Axial Compliance[a]

Material	R2	R3	R6
440C	0.095 (16.7)	0.091 (15.9)	0.028 (5.0)
Si_3N_4	0.081 (14.2)	0.066 (11.5)	0.022 (3.8)

[a] Compliance expressed as μm/N (μin/lb)

CONCLUSIONS

The use of Si_3N_4 gimbal bearings in this application appears worthy of further design study. The original magnetic and load capacity concerns are satisfactorily addressed using ceramic bearings and the preliminary study indicates the adhesive joint strength will be adequate, the compliance will be superior (stiffer), the bearing will react similarly to steel bearings as the load changes, and the Si_3N_4 pin will have adequate strength to survive the projected thermal stresses and moment loads. However, the concerns of pin strength, the strength of the thin outer ring when subjected to high bending loads, and the adhesive joint strength require further study, analysis, and test.

ACKNOWLEDGEMENTS

The authors wish to thank the Miniature Precision Bearing Division of MPB Corp. for support of the project and permission to publish the results. In addition the authors wish to thank John Lucek of Cerbec Ceramic Bearing Co. for providing useful data on the ceramic materials and several informative discussions. The authors also wish to thank Derek VanWyk and Adrian Wood of MPB for their assistance with the graphics and typesetting.

REFERENCES

1 Huntington Alloys (now Inco Alloys) data brochure "Inconel Alloy 600"

2 Courtesy of Cerbec Ceramic Bearing Company

3 American National Standard/Anti-friction Bearing Manufacturers Association Standard 9, Load Ratings and Fatigue Life for Ball Bearings, Section 3.8

4 Fujiwara, Yoshioka, Kitahara, Koizumi, Takabayashi, and Tada, Study on Load Rating Property of Silicon Nitride for Rolling Bearing Material, Journal of JSLE, Vol. 33, No. 4 (1988), P. 301

5 Private communication with John Lucek of Cerbec Ceramic Bearing Company

6 Komeya, K. and Kotani, H., Development of Ceramic Antifriction Bearing, JSAE Review, Vol. 7, No. 3, Page 72